IEEE Access
Multidisciplinary ⋮ Rapid Review ⋮ Open Access Journal

Received November 30, 2020, accepted December 8, 2020, date of publication December 10, 2020, date of current version December 23, 2020.

Digital Object Identifier 10.1109/ACCESS.2020.3043945

On Dynamic Service Chaining in Filterless Optical Metro-Aggregation Networks

LEILA ASKARI, OMRAN AYOUB, (Member, IEEE), FRANCESCO MUSUMECI, (Member, IEEE), AND MASSIMO TORNATORE, (Senior Member, IEEE)

Department of Electronics, Information and Bioengineering, Politecnico di Milano, 20133 Milan, Italy

Corresponding author: Leila Askari (leila.askari@polimi.it)

The work leading to these results has been supported by the European Community under grant agreement no. 761727 Metro-Haul Project.

ABSTRACT Filterless Optical Networks (FONs) in which optical nodes are formed by only passive splitters and combiners, are widely-adopted technical solution for transport networks, especially in the metro area, where relatively-low nodal degrees and limited link lengths allow to limit waste of wavelengths due to the broadcast nature of FONs. Up to now, FONs have been mostly deployed for scenarios where traffic requests are expected to be mostly static. However, considering emerging adoption of 5G services characterized by high traffic dynamics and thanks to recent advances in Network Function Virtualization, operators are now expected to perform more adaptive service provisioning and, consequently, dynamic network reconfiguration. In other words, it is possible to realize 5G services as Service Chains (SCs), using software components running on commodity servers in an agile way. In this work, we investigate the behavior of FONs under dynamic settings, considering that SC requests vary dynamically during the day. To this end, we provide an algorithm to perform dynamic service chaining in metro-aggregation networks, which considers the intrinsic wavelength broadcast nature in FONs. To provision services we need to allocate both computational and network resources to them. We consider two different traffic scenarios, with high dynamicity and low dynamicity, where the holding time of SCs ranges from a few seconds to a few minutes. Our illustrative numerical results, obtained using realistic network settings, show that FON architectures require the deployment of computational resources at all network nodes and the use of a filterless-aware SC provisioning algorithm to provide a performance in terms of provisioned bandwidth comparable to active optical networks. In particular, FONs (with additional investment in terms of computational resources) can outperform active networks under traffic with low dynamicity, while under high dynamic traffic FONs show acceptable performance slightly short of that of active networks.

INDEX TERMS Filterless optical networks, network function virtualization, service chaining.

I. INTRODUCTION

Filterless Optical Networks (FON) were first investigated more than a decade ago [1], but they are currently attracting the attention of operators as a low-cost technical solution to upgrade the capacity in optical Metro-Aggregation Networks (MAN) while averting excessive costs. In FONs, expensive Wavelength Division Multiplexing (WDM) layer active-switching devices, such as Re-configurable Optical Add-Drop multiplexers (ROADMs) based on Wavelength Selective Switches (WSS), are replaced by passive optical splitters and combiners. The absence of switching and filtering components in filterless nodes imposes a broadcast-and-select node operation [2], meaning that signals are broadcast to all outgoing ports of the filterless nodes, resulting in much higher spectrum consumption with respect to state-of-the-art ROADM-based optical networks.

In MANs, filterless nodes are often deployed in horse-shoe topologies (rings) along with WSS-based ROADMs terminal nodes deployed at horse-shoe ends that terminate signal broadcasting. Figure 1 shows the architecture of (a) a WSS-based terminal node, (b) a filterless node with splitters and combiners replacing WSSs, and (c) a scheme of a horse-shoe topology consisting of two active terminal nodes (i.e., nodes 1 and 2, colored red) and six filterless nodes (i.e., nodes 3 to 8, colored blue). Figure 1(c) shows also how two traffic demands (namely, from node 1 to node 8 and from node 8 to node 6) are routed in the filterless horse-shoe network, and

The associate editor coordinating the review of this manuscript and approving it for publication was Yang Tang.

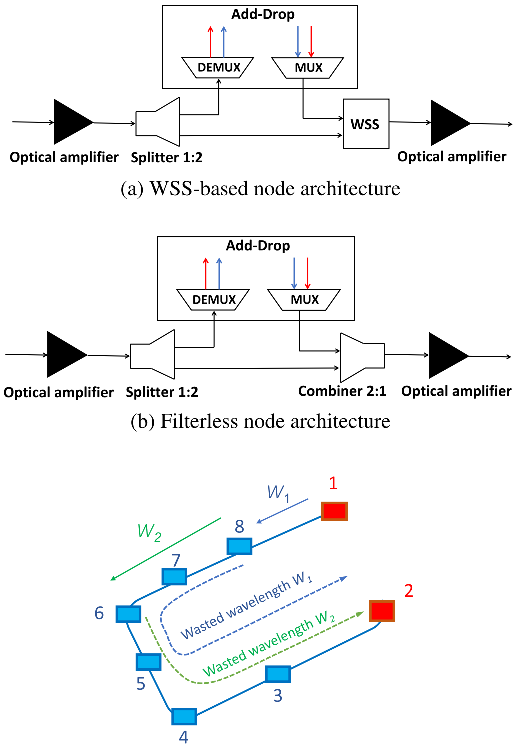

(a) WSS-based node architecture

(b) Filterless node architecture

(c) Wavelength waste

FIGURE 1. (a) Active and (b) Filterless node architectures. (c) An example of wavelength propagation due to broadcast-and-select architecture in a filterless network.

highlights signal propagation (signal waste) beyond destination due to broadcast in FON (respectively, wavelength W_1 on links between nodes 8 and 2 and wavelength W_2 on links between nodes 6 and 2). Note that W_1 and W_2 cannot be re-used on the horse-shoe to route traffic in the direction of node 2, a concept referred to as *no re-use* in FON, as re-using W_1 or W_2 will result in clash of wavelengths in the horse-shoe.

Despite spectrum waste, it has been shown that FON's design can be optimized to guarantee an acceptable performance in static traffic scenarios [3]. However, new services emerged in MANs, which require network operators to dynamically reconfigure network resource allocation to agilely provision new 5G services. To this end, Network Function Virtualization (NFV) as a new paradigm was introduced. NFV replaces hardware devices with software instances named Virtual Network Function (VNF), that can be run on commodity hardware and are connected in a specific sequence to form a Service Chain (SC), which provides a service to users.

Therefore, to cope with the arrival of new highly dynamic 5G services, FONs must be properly deployed to avoid excessive spectrum waste in presence of dynamic traffic. Note that, in FONs, signals might propagate beyond the destination node of a connection, resulting in spectrum waste, and changing wavelength assignment of demands too often may result in even larger spectrum waste. Furthermore, filterless nodes provide less flexibility and re-configurability with respect to nodes with filtering capabilities [4], therefore, they have been traditionally considered more suitable for static traffic scenarios.

In this paper, we investigate the problem of service provisioning in filterless MANs under dynamic traffic. We consider a MAN with NFV-enabled mini-data center nodes (NFV-nodes) capable of provisioning and terminating services. In particular, we devise algorithms for SC provisioning in filterless MANs and compare their performance to that of an active network considering investments at different layers, i.e., at the WDM layer as well as at the network equipment and computational (i.e., IT) resources deployed in NFV-nodes. Note that, the number of NFV-nodes affects the performance of the algorithm and at the same time the total cost of the network. In other words, increasing number of NFV-nodes will lead to having more flexibility in deciding about the placement of VNFs and where to terminate the SC, however, network operators need to invest more to equip more NFV-nodes with computational resources. The contributions of the paper can be summarized as follows:

- We formally state the problem of dynamic service chaining in filterless optical MANs.
- We propose an algorithm to perform resource-aware dynamic SC provisioning in FON, which is developed using a discrete-event-based simulator
- We perform experimental simulations to compare the performance of a FON to that of active networks, as well as the performance of our proposed algorithm to that of baseline algorithms in FONs considering different amount of investments in computational resources (i.e., different number of NFV-nodes to host NFV instances in the network), under low dynamic and high dynamic traffic scenarios.

The rest of the paper is organized as follows. Section II discusses related work on FONs and dynamic service chaining. Section IV formally states the problem of dynamic service chaining in FONs and describes the algorithms proposed to solve it. Section V discusses illustrative numerical results. Section VI concludes the paper.

II. RELATED WORK

Studies on dynamic service chaining [5] have already appeared in literature, however none of them specifically focus on FON architectures. In [6] different algorithms are proposed to dynamically provision SCs satisfying their bandwidth, computing and end-to-end latency requirements in distributed datacenters. In [7], the authors provide an Integer Linear Programming (ILP) model to perform dynamic VNF placement considering load on NFV-nodes. They also provide a heuristic algorithm for dynamic relocation of VNFs considering CPU and memory resource requirements of VNFs. In addition, performance of their proposed algorithms are evaluated on a testbed. Authors of [8] use reinforcement learning to provide online fault tolerant VNF placement solution. Ref. [9] provides an ILP formulation for online VNF placement using a forwarding graph, with the objective of minimizing VNF reconfigurations, while satisfying Quality of Service (QoS). In [10], authors provide an online two-step algorithm to decide the optimal number and location of VNFs in large datacenters networks depending on required bandwidth and CPU resources. Ref. [11] proposes an algorithm for online traffic routing with the objective of achieving optimal trade off between throughput and meeting QoS requirements of users by deciding about accepting or rejecting a flow request based on current state of the network.

Concerning FONs, early works concentrated on meshed regional-core networks. The resource allocation problem in FONs typically includes the routing and wavelength/spectrum assignment and the establishment of fiber trees, i.e., loop-free fiber coverage interconnecting add/drop traffic nodes, to prevent undesired laser-loop effects due to continuous signal broadcasting and amplification [1], [12], [13]. Other works, such as Refs. [14] and [15], investigated the placement of programmable optical switches and filters at specific network nodes to reduce spectrum consumption in fiber-tree based FONs. More recent works, such as [3], investigate the problem of virtual network embedding in FONs, however also considering static traffic and focusing on core networks. With respect to these works, our study focuses on metro networks and considers dynamic traffic scenario which requires different approaches than those previously proposed.

The interest in applications of FONs in MANs has increased significantly in the recent years [16], [17]. For example, Ref. [17] investigated FON deployment cost in MANs and Ref. [18] devised a techno-economic cost model that included capital and operational expenditure of FONs and compared it to that of active photonic networks. Results show that FONs can help reduce the cost of optical layer by 5% to 10% in metro networks. Ref. [19] showed that further savings can be achieved due to lower cost of data and control planes for filterless networks. Ref. [20] devised a Software Defined Network-enabled control plane for dynamic filterless metro networks however not considering the SC provisioning problem. Moreover, Ref. [21] investigated optimizing DC resources at metro-edge nodes while taking into consideration optical transponder costs and service latency in filterless networks, however this work considered a static traffic scenario and did not consider the VNF deployment problem. To the best of our knowledge, no previous work investigated the problem of VNF placement and dynamic service chaining in filterless optical metro networks.

III. DYNAMIC SERVICE CHAINING IN FILTERLESS OPTICAL MAN

The problem of dynamic service chaining in filterless optical MAN can be stated as follows. Given a filterless optical MAN where fiber trees are established, for each dynamically-arriving SC request we decide the placement of its VNFs along with the SC traffic routing and wavelength assignment, with the objective of maximizing the total provisioned bandwidth in the network, subject to the ''no-re-use'' constraint in FONs. To provision a SC we need to place the VNFs on nodes equipped with computational capacity (referred to as NFV-nodes). However, due to frequency re-use restriction in FON, we are not always able to utilize all the NFV-nodes in the network. In other words, there might be a situation in which an NFV-node has enough computational capacity but is not accessible simply because all the wavelengths on the links connected to this NFV-node are occupied. Therefore, the mapping of VNFs to NFV-nodes should be done in a way to minimize the impact of frequency re-use restriction. To this end, we try to consolidate all VNFs belonging to a SC on a single node as much as possible and preferably on the node where the SC is terminated(destination node of the SC). In this way, we are able to provision the SC request in the network by using as few as possible wavelengths.

Figure 2 shows an example of different provisioning strategies for a SC consisting of two VNFs (namely, *VNF1* and *VNF2*), and the resulting wavelength utilization in an active network (subfigure a) and in a filterless network (subfigures b-d). In Figure 2(a), both *VNF1* and *VNF2* are placed at node *3* (the only NFV-node), resulting in wavelength *W1* being used on links *4-3*, *3-2* and *2-1*, i.e., a total occupation of 3 units of capacity (one wavelength on three links). In Figure 2(b), the same VNF mapping as in 2(a) is performed, but considering a filterless network; in this case, traffic routed between node *4* and node *3* is transported using wavelength *W1* (note that *W1* is wasted on links *3-2* and *2-1*, due to the broadcast nature of filterless nodes) and traffic routed between nodes *3* and *1* is assigned wavelength *W2*, resulting in the usage of two wavelengths occupying a total of 5 units of capacity (2 of which are wasted) on all links. Moreover, Figure 2(c) shows how having more NFV-nodes (i.e., more possible locations to place VNFs) and optimizing the placement of VNFs allow to reduce the overall wavelength utilization in a filterless network (4 wavelengths are occupied on all links instead of 5 in Figure 2(b)). Note that, even if more NFV-nodes are present in the network, a non-optimized VNF placement, such as the case of Figure 2(d), might result in excessive spectrum utilization (total of 6 wavelengths occupied). This example shows that (1) additional investment in terms of computational resources (more NFV-nodes) and (2) a filterless-aware SC provisioning are required to avert excessive wavelength consumption in a filterless network. Note that deploying more NFV-nodes in a filterless network than that in an active network does not necessarily translate into higher overall investment as the filterless network provides significant cost savings at the WDM layer.

IV. DYNAMIC SERVICE CHAINING ALGORITHMS

In this section, we first describe the proposed SC provisioning algorithm in FON, namely, *filterless-aware dynamic SC provisioning algorithm* (*FVNFP*), and then present the algorithm considered for dynamic SC provisioning in active networks.

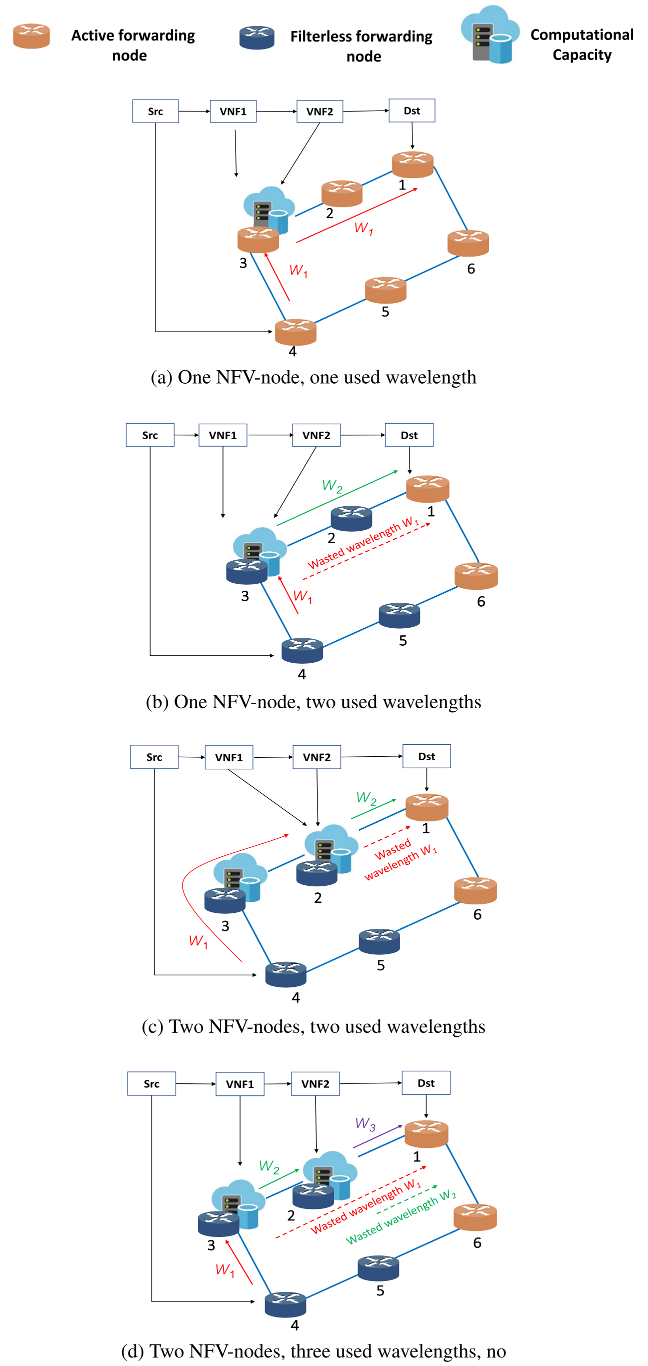

(a) One NFV-node, one used wavelength

(b) One NFV-node, two used wavelengths

(c) Two NFV-nodes, two used wavelengths

(d) Two NFV-nodes, three used wavelengths, no consolidation

FIGURE 2. Different VNF mapping strategies.

A. FILTERLESS-AWARE DYNAMIC SC PROVISIONING ALGORITHM

FVNFP algorithm takes as input the following parameters:

- $G(N,E)$: Current state of the network, where N indicates the set of nodes in the network and E is the set of bidirectional fiber links
- F: Set of NFV-nodes in the network ($F \subseteq N$)
- V: Set of all possible VNFs which constitute the service requests
- S: Types of SCs to be deployed
- W: Number of wavelengths for each link in the network
- T: Set of fiber trees in the network
- r: SC request specified by:
  - S_r: Source node of the SC request
  - D_r: Destination node of the SC request
  - $N_{vnf,r}$: Number of VNFs forming the SC
  - V_r: VNFs used by the SC ($V_r \in V$)
  - L_r: Latency tolerated by users of the SC
  - B_r: Bandwidth requirements of SC
  - H_r: Holding time of SC request
  - NU_r: Number of users for the SC

FVNFP is a modified version of our previously proposed algorithm for dynamic VNF placement in active photonic networks [22], which we adapted to the characteristics and requirements of filterless MANs. The pseudocode of *FVNFP* algorithm is shown in *Algorithm* 1 and it consists of two phases. In the first phase, as shown in line 4, upon arrival of a SC request r, *FVNFP* first calculates the shortest path between source S_r and destination D_r of SC request ($SP_{S,D}$). After that, algorithm chooses the next VNF from V_r that needs to be mapped on an NFV-node. If $SP_{S,D}$ is available, in line 6 *FVNFP* checks whether D_r has enough CPU resources for V_r' requested by NU_r users or not. In case the node has enough computational resources, this node is chosen as NFV-node to map V_r' and the computational resources of the node is updated. After that, the next V_r' is chosen to be mapped in the network. These steps are shown in lines 7 to 9. If this is not the case, V_r' will be mapped on an NFV-node along the $SP_{S,D}$ with enough computational capacity. If such node is found, in lines 11 to 14, algorithm will map V_r' to this node (F) and update the computational capacity of F and *FVNFP* will choose the next V_r' to map. If this is not the case, *FVNFP* lists all NFV-nodes in F based on their distance from S_r and chooses closest NFV-node to S_r with enough CPU resources. In case such node is not found, r is blocked, otherwise the computational resources of this node will be updated and algorithm will decide about the placement of next $V_r' \in V_r$. These steps are depicted in lines 20 to 24. The above-mentioned steps are repeated until either all $V_r' \in V_r$ are mapped or r is blocked. After deciding the VNFs' placement, wavelength assignment is performed in the second phase of *FVNFP*. These steps are shown in lines 28 to 46. For each link L belonging to the path of SC request r (r_{Path}), if L is a link on one of the fiber trees in the network, *FVNFP* at line 31 at first tries to find a wavelength W that is not assigned to any other SC request currently active in the network on this fiber tree. If such W is found, this wavelength will be invalidated on the fiber tree that L belongs to (T_L). If this is not the case, the SC request will be blocked. For all other links L in r_{Path} that do not belong to T_L, i.e., are connected to the active nodes, *FVNFP* in line 38 tries to find a W with enough free capacity to accommodate r. If such W is found, the bandwidth resources on W are allocated to r and free capacity of W is updated. If this is not the case, r will be blocked.

B. DYNAMIC SC PROVISIONING IN ACTIVE PHOTONIC NETWORKS

As a dynamic VNF placement algorithm for active networks, we consider *Dynamic VNF Placement* (*DVNFP*) algorithm proposed in our previous work [22]. *DVNFP* performs dynamic VNF placement and routing and wavelength assignment with the aim of maximizing the number of SC requests provisioned and minimizing the number of NFV-nodes and latency-violated SCs in the network. We apply *DVNFP* in active networks as it proved to provide better performance compared to baseline algorithms [22]. Moreover, we apply *DVNFP* in filterless networks with the aim of evaluating the advantages our filterless-aware algorithm, *FVNFP*, provides with respect to an algorithm not adapted for filterless networks.

C. ALGORITHM's COMPLEXITY

To calculate the shortest path in our algorithm we use Dijkstra's algorithm. Considering that, to implement Dijkstra's algorithm, we used binary heaps (an efficient data structure for fast Dijkstra's computation), the order of computational complexity for line 4 is $O(N + E \log N)$. In addition, the complexity for line 3 is in the order of $O(|V_r|)$. As for the second phase of *FVNFP* the computational complexity is in the order of $O(|r_{path}|)$. Therefore, *FVNFP* has the complexity that is in the order of $O(|V_r|[N + E \log N])$.

Algorithm 1 Filterless-Aware VNF Placement (FVNFP)

1: Given:network state *G(N,E)* and set of NFV-nodes F, Set of fiber trees T, Set of VNFs V, Service Chain request $r(S_r, D_r, N_{vnf,r}, V_r, L_r, B_r, H_r)$
2: **repeat**
3: $V_r' \leftarrow$ Select the next VNF $\in V_r$
4: $SP_{S,D} \leftarrow shortestpath(S_r, D_r)$
5: **if** $\exists SP_{S,D}$ **then**
6: **if** $D_{CPU} > CPUReq(V_r', NU_r)$ **then**
7: Place V_r' on D_r
8: $D_{CPU} \leftarrow D_{CPU} - CPUReq(V_r', NU_r)$
9: goto 3
10: **else**
11: Place V_r' on $F \in SP_{S,D}$ **where** $F_{CPU} > CPUReq(V_r', NU_r)$
12: **if** Success **then**
13: $F_{CPU} \leftarrow F_{CPU} - CPUReq(V_r', NU_r)$
14: goto 3
15: **else**
16: goto 20
17: **end if**
18: **end if**
19: **else**
20: Choose $f \in F$ **where** Dist(f,S_r) is minimum & $f_{CPU} > CPUReq(V_r', NU_r)$
21: **if** Success **then**
22: goto 3
23: **else**
24: **return** *r blocked*
25: **end if**
26: **end if**
27: **until** all VNFs $\in V_r$ are placed and chained
▷ Phase 2: Wavelength assignment
28: **For each** $L \in r_{Path}$
29: **repeat**
30: **if** $L \in T_L$ **then**
31: Find a $W \in L$ **where** W is not currently used on T_L
32: **if** $\nexists$ W **then**
33: **return** *r blocked*
34: **else**
35: invalidate W on all $l \in T_L$
36: **end if**
37: **else**
38: Find a $W \in L$ **where** $FreeCap(W) > B_r$
39: **if** $\nexists$ W **then**
40: **return** *r blocked*
41: **else**
42: $FreeCap(W) \leftarrow FreeCap(W) - B_r$
43: **end if**
44: **end if**
45: **until** all $L \in r_{Path}$ are mapped
46: **return** *r provisioned*

V. NUMERICAL RESULTS

In this section, we discuss numerical results comparing the performance of SC provisioning algorithm in a filterless network to that of an active network under dynamic traffic.

A. NETWORK SCENARIOS

We perform the analysis considering different scenarios, i.e., different network architectures, different number of NFV-nodes in the network as well as different VNF placement algorithms. Overall, we consider the following different network scenarios:

- *DVNFP-FON-all*: In this scenario, we use *DVNFP* algorithm to perform SC provisioning. This network is a FON where all the nodes in the network are NFV-nodes.
- *FVNFP-FON-all*: In this scenario, we use *FVNFP* algorithm in a FON network where all the nodes are considered to be NFV-nodes.
- *DVNFP-FON-half*: In this scenario, we use *DVNFP* algorithm to perform SC provisioning. This network is a FON where half of the nodes in the network are NFV-nodes.
- *FVNFP-FON-half*: In this scenario, *FVNFP* algorithm is used in a FON with half of the nodes considered as NFV-nodes.
- *DVNFP-Active-half*: In this scenario, we use *DVNFP* algorithm for SC provisioning in an active network using half of the nodes in the network as NFV-nodes.

Note that since *FVNFP* is designed for FONs, we will not compare its performance in active networks. In all network scenarios, we consider that each NFV-node in the network is equipped with 24 CPU cores (VCPU). Table 1 summarizes

TABLE 1. Characteristics of the five network scenarios considered in our study.

Network Architecture	Algorithm	Nr. NFV-nodes	Network Scenario
Filterless	FVNFP	26	FVNFP-FON-half
		51	FVNFP-FON-all
	DVNFP	26	DVNF-FON-half
		51	DVNFP-FON-half
Active	DVNFP	26	DVNFP-Active-half

the characteristics of the different network scenarios considered.

For the active network scenario *DVNFP-Active-half*, all network nodes are active nodes (WSS-based ROADM) while for the filterless network scenarios the terminal nodes are active nodes (colored in red) while the rest are filterless nodes (colored in blue). We compare the performance of the network scenarios in terms of:

- *Provisioned bandwidth* (B_h), that is calculated as the summation of the bandwidth request for provisioned SCs at each hour.

$$B_h = \sum\nolimits_{SC \in SC_{prov}} B_{SC} \tag{1}$$

- *Latency violation ratio* that is the ratio of SC requests that their latency requirement is not satisfied (SC_V) out of total of provisioned SCs (SC_{tot}) at each hour.

$$LV_h = \frac{SC_V}{SC_{tot}} \tag{2}$$

- *Average number of active NFV-nodes* that is calculated considering number of NFV-nodes having at least one running instance of a VNF averaged by the duration of each SC calculated for each hour.

$$N_{avg,h} = \sum\nolimits_{SC \in SC_{prov}} \frac{N_{SC} \cdot t_{SC}}{t_{tot}} \tag{3}$$

B. SIMULATION SETTINGS AND SERVICE CHAIN MODELING

To perform dynamic simulations, we develop a C++ discrete event-based driven simulator. As network topology, we consider 51-node MAN topology depicted in Figure V-B. We consider that each fiber supports 12 wavelengths with 1 Gbps capacity. We used synthetic traffic profile for 24 hours, taken from [23], as illustrated in Figure 4. The SC requests are generated according to Poisson distribution with average arrival rate following the traffic profile in Figure 4. Note that, we consider two different traffic scenarios in our simulations, namely, *high dynamicity* and *low dynamicity*. In *high dynamicity* scenario, SC requests arrive dynamically at each hour with an arrival rate λ_h and stay for a short amount of time in the network (low holding time with an average duration of T_h equal to 5 seconds) and then leave. In *low dynamicity* scenario, SC requests have higher holding time, meaning that they stay longer in the network (average holding time of $T_l = 250$ seconds) but with an arrival rate that is 50 times lower than that of the *high dynamicity* scenario ($\lambda_l = \frac{\lambda_h}{50}$), resulting in the same offered traffic for both traffic scenarios ($T_h \cdot \lambda_h = T_l \cdot \lambda_l$).

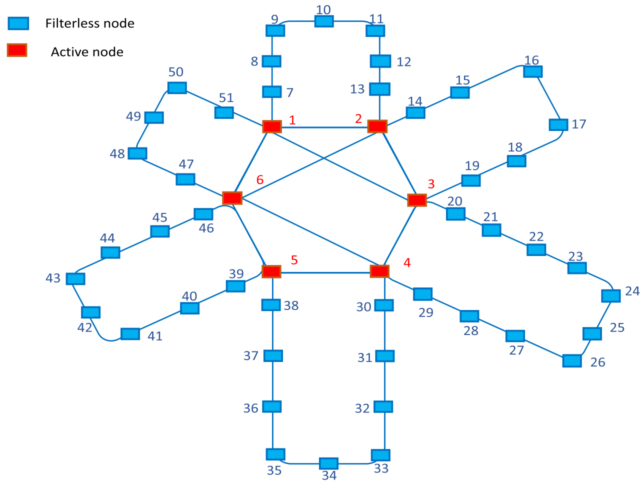

FIGURE 3. Metro-aggregation network topology considered in our study.

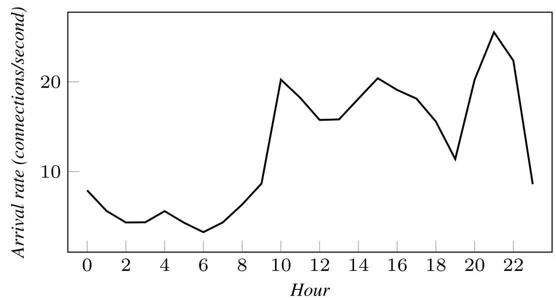

FIGURE 4. Traffic profile.

TABLE 2. Service chains with corresponding VNFs, bandwidth and latency characteristics.

Service Chain	Service Chain VNFs	Bandwidth	Latency
Augmented Reality	NAT-FW-TM-VO-IDS	100 Mbps	1 ms
MIoT	NAT-FW-IDS	100 Mbps	5 ms
Smart Factory	NAT-FW	100 Mbps	1 ms

Table 2 reports the different SCs considered in our simulations and their bandwidth and latency requirements and Table 3 reports the computational requirements of each of the VNFs. We consider that the source and destination nodes of a SC can be chosen randomly in the network. However, we assume that Augmented Reality and Massive IoT (MIoT) SC types can be terminated at any NFV-node, while the Smart Factory SC is forced to be terminated (i.e., is forced to have its destination node) at the Core CO.

C. DISCUSSION

1) LOW DYNAMICITY

We first compare the performance of the different network architectures in the low dynamicity scenario, i.e., the case in which the dynamically arriving SC requests, in each hour during the day, stay for only few minutes in the network. Figure 5(a) shows the provisioned bandwidth (Mbps) with respect to time of the day. Overall, results show that

TABLE 3. CPU core usage for VNFs.

VNF Name	NAT	FW	VO	TM	IDS
CPU Core	0.0184	0.018	0.108	0.266	0.214

FVNFP-FON-all and *DVNFP-Active-half* achieve almost the same performance, with a slight variation during low offered traffic and high offered traffic. In particular, during low offered traffic (from hour 0 to hour 9), *DVNFP-Active-half* performs slightly better than *FVNFP-FON* (4% more provisioned bandwidth), while during hours of high offered traffic (between hour 9 and hour 23), *FVNFP-FON-all* shows better performance with respect to *DVNFP-Active-half* provisioning up to 10% more bandwidth. This shows that in a FON, investing more on computational resources is decisive to achieve the desired performance. Indeed, *FVNFP-FON-half*, with 26 NFV-nodes shows a bad performance compared to *FVNFP-FON-all* and *DVNFP-Active-half* provisioning only 50% of the bandwidth. Moreover, results show that employing a proper filterless-aware VNF placement algorithm adapted to the requirements of FONs has a key role as *FVNFP-FON-all* achieves significantly higher provisioned bandwidth than *DVNFP-FON-all*, which provisions only 40% of the bandwidth provisioned by *FVNFP-FON-all* at some hours of the day.

Figure 5(b) illustrates the average number of active NFV-nodes in each network scenario. We can observe that the number of NFV-nodes for all scenarios, regardless of the traffic, remains constant. Specifically, for *FVNFP-FON-all*, almost half of the NFV-nodes remain active while for *DVNFP-Active-half* 18 nodes remain active. This is due to the fact that, in this scenario, SCs have higher holding time, and consequently NFV nodes need to be active for longer time on average. This outcome further shows that *FVNFP-FON-all* incurs significantly higher power consumption due to the computational resources with respect to *DVNFP-Active-half*, depriving FON from one of its main advantages, which is the low operational power due to the deployment of passive optical devices.

As for the latency violation ratio, it is observed only in *DVNFP-Active-half* during hours of high offered traffic. This is because, when links are congested, SCs are provisioned from NFV-nodes far from destination, adding up to the switching latency present in the active network due to WSSs, an aspect that is not experienced in FON.

2) HIGH DYNAMICITY

We now compare the performance of the different network scenarios in the high dynamicity scenario. Figure 6(a) plots the provisioned bandwidth of each of the network scenarios (in Mbps) with respect to time of the day. Results show that, overall, in terms of provisioned bandwidth, *DVNFP-Active-half* and *FVNFP-FON-all* perform better than all other network scenarios (i.e., better than the rest FON scenarios), with *DVNFP-Active-half* showing slightly better performance than *FVNFP-FON-all*. In particular, at low offered traffic (from hour 0 till hour 9), *DVNFP-Active-half* and *FVNFP-FON–all* show the same performance, and they provision up to 10% more bandwidth with respect to *FVNFP-FON-half* and 50% more bandwidth with respect to *DVNFP-FON-all* and *DVNFP-FON-half*. At higher offered traffic (i.e., from hour 10 to hour 23), *DVNFP-Active-half* shows better performance than *FVNFP-FON-all*, provisioning 5% to 10% more bandwidth. The performance

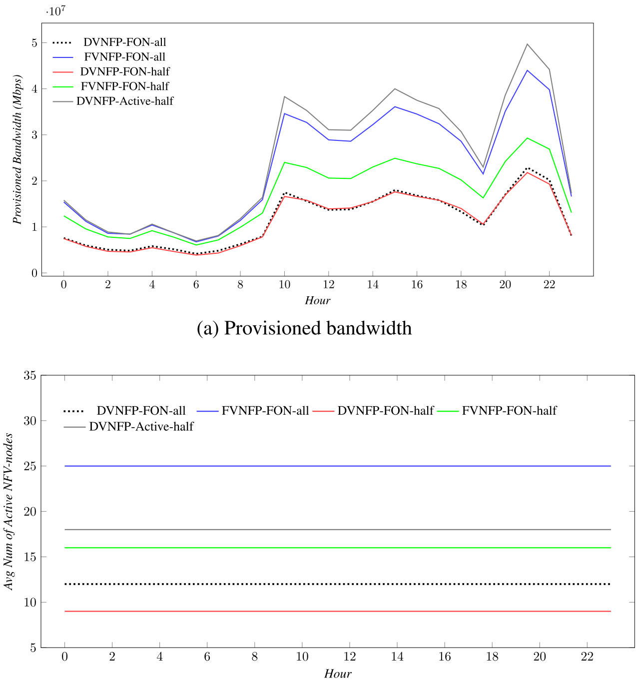

(a) Provisioned bandwidth

(b) Average number of active NFV-nodes

FIGURE 5. Simulation results for low dynamicity network setting.

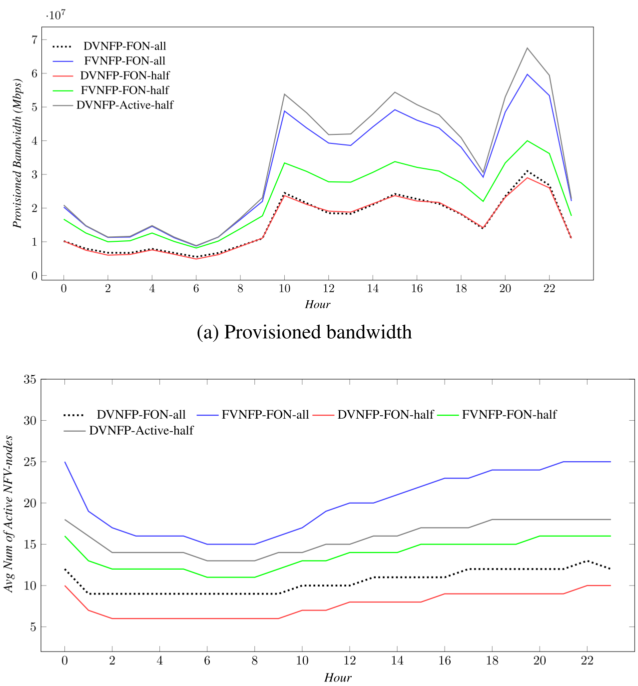

(a) Provisioned bandwidth

(b) Average number of active NFV-nodes

FIGURE 6. Simulation results for high dynamicity network setting.

of other network scenarios is further worsened with respect to that of *DVNFP-Active-half* and *FVNFP-FON-all*. For instance, *FVNFP-FON-half* provisions between 50% and 60% that of *DVNFP-Active-half* while *DVNFP-FON-all* and *FVNFP-FON-half*, which show same performance, provision 35% and 45% that of *DVNFP-Active-half*. Results also show that *DVNFP-FON-half* and *DVNFP-FON-all* show the same performance. In other words, increasing the number of NFV-nodes in a FON network from 26 to 51 while using *DVNFP* algorithm (comparing *DVNFP-FON–half* and *DVNFP-FON–all*), has no impact on network performance. However, using filterless-aware algorithm (*FVNFP*) instead of *DVNFP*, the provisioned bandwidth increases up to 42%. These results allow to conclude that, under highly dynamic traffic scenarios, 1) additional investment in terms of NFV-nodes is required in FON architecture and 2) the use of filterless-aware SC provisioning algorithm (i.e., *FVNFP*) is essential to maintain an acceptable performance in terms of provisioned bandwidth in Filterless-based MAN architecture.

Figure 6(b) plots the average number of active NFV-nodes for each of the network scenarios. Results show that *FVNFP-FON-all* utilizes the highest average number of NFV-nodes among all network scenarios however, although 51 NFV-nodes are present in *FVNFP-FON-all* network scenario, the number of average NFV-nodes utilized by *FVNFP-FON-all* ranges between 16 and 25 only. Compared to that of *DVNFP-Active-half*, which ranges between 14 and 23, *FVNFP-FON-all* utilizes slightly more NFV-nodes, between 2 and 7 NFV-nodes (14% and 30%). This shows that the operational expenditure of NFV-nodes in the *FVNFP-FON-all* is only slightly higher than that of *DVNFP-Active-half*, in-spite of the fact that in *FVNFP-FON-all* almost double the number of NFV-nodes are deployed with respect to *DVNFP-Active-half*. The fact that a relatively high percentage of the nodes require to be NFV-nodes (as otherwise performance in terms of provisioned bandwidth is not acceptable (*FVNFP-FON-half* in Figure 6(a))) while only around 50% of them are active means that double the capital investment in terms of computational power is required in a FON architecture with respect to that of an active (51 NFV-nodes instead of 26) but only a slight increase in terms of operational power is expected. Put differently, a FON architecture requires a relatively high number of NFV-nodes to perform better placement of VNFs, and therefore to avoid excessive waste of wavelengths, yet it does not incur significant operational costs than that of active, which adds up to the advantages FON provides in terms of operational expenditure on the optical WDM layer. Note that further cost savings of computational power in FON architecture are possible if number, location and capacity of NFV-nodes are jointly optimized, however we leave this aspect for future work as it falls beyond the scope of this study.

As for the latency violation, it occurs only for high offered traffic in *DVNFP-Active-half*. This is because when network is congested, the closest NFV-nodes to the source of SC request are not reachable, and therefore, VNFs are placed in NFV-nodes far in the network. Although network congestion also happens in filterless networks, latency violation is avoided due to the absence of electrical-optical conversions, unlike for active network architectures.

D. SUMMARY

This subsection summarizes the main takeaways drawn by the numerical comparison of the two main network scenarios, a FON network where all network nodes are NFV-nodes and an active network with half of the network nodes being NFV-nodes.

In a traffic scenario with low traffic dynamicity, FON with all nodes functioning as NFV-nodes shows a comparable performance to an active optical network with only half of the network nodes acting as NFV-nodes in terms of provisioned bandwidth. In terms of average number of active NFV-nodes, FON solution shows a disadvantage as it requires almost double the number of active NFV-nodes of that of an active network, which translates into operational expenditure of computational power and reduces the overall operational expenditure savings expected in FON due to the replacing WSS-based ROADMs by passive devices.

In a traffic scenario with high dynamicity, FON shows an acceptable performance in terms of provisioned bandwidth however it is slightly outperformed by the active network architecture. In terms of NFV-nodes, the FON, despite having double the number of NFV-nodes deployed, has an average number of active NFV-nodes only slightly higher than that of the active network architecture, which promises overall savings in operational expenditure due to the use of passive optical devices instead of active devices in the WDM layer.

VI. CONCLUSION

We focus on the problem of dynamic SC provisioning in filterless MAN. For this aim, we develop a discrete event-based simulator and propose a filterless-aware VNF placement algorithm for SC provisioning in filterless MAN. We then perform dynamic simulations and evaluate the performance of FON comparing it to that of an active network in terms of provisioned bandwidth, number of active NFV-nodes and latency violation. In particular, we evaluate the performance of FON considering different number of NFV-nodes deployed in the network. Results obtained show that FON is suitable for dynamically provisioning SCs only when all network nodes are equipped with computational resources and while employing our proposed SC provisioning algorithm adapted to the characteristics of FONs. Furthermore, results show that FONs, in a traffic scenario with low dynamicity, when all network nodes are equipped with computational capacity, show a better performance than that of active networks. In a traffic scenario with high dynamicity, and even if all nodes are equipped with computational capacity, FON is outperformed by an active network architecture yet it shows an overall acceptable performance in terms of provisioned bandwidth and promises significant savings in terms of operational expenditure.

REFERENCES

[1] É. Archambault, D. O'Brien, C. Tremblay, F. Gagnon, M. P. Bélanger, and É. Bernier, "Design and simulation of filterless optical networks: Problem definition and performance evaluation," *IEEE/OSA J. Opt. Commun. Netw.*, vol. 2, no. 8, pp. 496–501, Aug. 2010.

[2] C. Tremblay, A. Enriquez-Castillo, M. P. Belanger, and F. Gagnon, "Filterless WDM optical core networks based on coherent systems," in *Proc. 13th Int. Conf. Transparent Opt. Netw.*, Jun. 2011, pp. 1–4.

[3] O. Ayoub, L. Askari, A. Bovio, F. Musumeci, and M. Tornatore, "Virtual network mapping vs embedding with link protection in filterless optical networks," in *Proc. IEEE Global Commun. Conf. (Globecom)*, Sep. 2020, pp. 1–6.

[4] *The Metro-Haul Project Deliverables*. Accessed: Aug. 1, 2019. [Online]. Available: https://metro-haul.eu/deliverables/

[5] J.-J. Pedreno-Manresa, P. S. Khodashenas, J.-L. Izquierdo-Zaragoza, and P. Pavon-Marino, "Improved user experience by dynamic service handover and deployment on 5G network edge," in *Proc. 21st Int. Conf. Transparent Opt. Netw. (ICTON)*, Jul. 2019, pp. 1–4.

[6] S. Fichera, R. Martínez, B. Martini, M. Gharbaoui, R. Casellas, R. Vilalta, R. Muñoz, and P. Castoldi, "Latency-aware resource orchestration in SDN-based packet over optical flexi-grid transport networks," *J. Opt. Commun. Netw.*, vol. 11, no. 4, p. B83, 2019.

[7] T. Mahboob, Y. R. Jung, and M. Y. Chung, "Dynamic VNF placement to manage user traffic flow in software-defined wireless networks," *J. Netw. Syst. Manage.*, vol. 28, pp. 1–21, Mar. 2020.

[8] W. Mao, L. Wang, J. Zhao, and Y. Xu, "Online fault-tolerant VNF chain placement: A deep reinforcement learning approach," in *Proc. IFIP Netw. Conf. (Networking)*, 2020, pp. 163–171.

[9] N. T. Jahromi, S. Kianpisheh, and R. H. Glitho, "Online VNF placement and chaining for value-added services in content delivery networks," in *Proc. IEEE Int. Symp. Local Metrop. Area Netw. (LANMAN)*, Jun. 2018, pp. 19–24.

[10] G. Moualla, T. Turletti, and D. Saucez, "Online robust placement of service chains for large data center topologies," *IEEE Access*, vol. 7, pp. 60150–60162, 2019.

[11] L. Guo, J. Pang, and A. Walid, "Dynamic service function chaining in SDN-enabled networks with middleboxes," in *Proc. IEEE 24th Int. Conf. Netw. Protocols (ICNP)*, Nov. 2016, pp. 1–10.

[12] B. Jaumard, Y. Wang, and N. Huin, "Optimal design of filterless optical networks," in *Proc. 20th Int. Conf. Transparent Opt. Netw. (ICTON)*, Jul. 2018, pp. 1–5.

[13] M. Gunkel, A. Mattheus, F. Wissel, A. Napoli, J. Pedro, N. Costa, T. Rahman, G. Meloni, F. Fresi, F. Cugini, N. Sambo, and M. Bohn, "Vendor-interoperable elastic optical interfaces: Standards, experiments, and challenges [invited]," *J. Opt. Commun. Netw.*, vol. 7, no. 12, p. B184, 2015.

[14] V. Abedifar and M. Eshghi, "Routing, modulation format, spectrum and core allocation in space-division-multiplexed programmable filterless networks," *Opt. Fiber Technol.*, vol. 49, pp. 37–49, May 2019.

[15] O. Ayoub, F. Fatima, A. Bovio, F. Musumeci, and M. Tornatore, "Traffic-adaptive re-configuration of programmable filterless optical networks," in *Proc. IEEE Int. Conf. Commun. (ICC)*, Jun. 2020, pp. 1–6.

[16] F. Paolucci, R. Emmerich, A. Eira, N. Costa, J. Pedro, P. W. Berenguer, C. Schubert, J. K. Fischer, F. Fresi, A. Sgambelluri, and F. Cugini, "Disaggregated edge-enabled C+L-band filterless metro networks," *IEEE/OSA J. Opt. Commun. Netw.*, vol. 12, no. 3, pp. 2–12, Mar. 2020.

[17] C. Tremblay, É. Archambault, M. P. Bélanger, P. Littlewood, W. Clelland, M. Furdek, and L. Wosinska, "Agile optical networking: Beyond filtered solutions," in *Proc. Opt. Fiber Commun. Conf.*, 2018, pp. 1–3.

[18] O. Karandin, O. Ayoub, F. Musumeci, and M. Tornatore, "A techno-economic comparison of filterless and wavelength-switched optical metro networks," in *Proc. 22nd Int. Conf. Transparent Opt. Netw. (ICTON)*, 2020, pp. 1–6.

[19] P. Pavon-Marino, F.-J. Moreno-Muro, M. Garrich, M. Quagliotti, E. Riccardi, A. Rafel, and A. Lord, "Techno-economic impact of filterless data plane and agile control plane in the 5G optical metro," *J. Lightw. Technol.*, vol. 38, no. 15, pp. 3801–3814, Aug. 1, 2020.

[20] E. Kosmatos, D. Uzunidis, C. Matrakidis, A. Stavdas, S. Horlitz, T. Pfeiffer, and A. Lord, "Building a truly dynamic filterless metro network by reusing a commercial PON's data-plane and a novel SDN-enabled control-plane," *J. Lightw. Technol.*, vol. 37, no. 24, pp. 6033–6039, Dec. 15, 2019.

[21] A. Eira and J. Pedro, "The role of metro transport node architectures in optimized edge data-center dimensioning," in *Proc. Int. Conf. Opt. Netw. Design Modeling (ONDM)*, May 2020, pp. 1–6.

[22] L. Askari, A. Hmaity, F. Musumeci, and M. Tornatore, "Virtual-network-function placement for dynamic service chaining in metro-area networks," in *Proc. Int. Conf. Opt. Netw. Design Modeling (ONDM)*, May 2018, pp. 136–141.

[23] M. Gattulli, M. Tornatore, R. Fiandra, and A. Pattavina, "Low-emissions routing for cloud computing in IP-over-WDM networks with data centers," *IEEE J. Sel. Areas Commun.*, vol. 32, no. 1, pp. 28–38, Jan. 2014.

LEILA ASKARI received the M.Sc. degree in telecommunication engineering from Politecnico di Milano, Milan, Italy, in October 2017, where she is currently pursuing the Ph.D. degree in information technology. Her research interests mainly focus on network function virtualization and specifically virtual network function placement.

OMRAN AYOUB (Member, IEEE) received the M.Sc. and Ph.D. degrees from Politecnico di Milano, Milan, Italy, in 2015 and 2019, respectively. He is currently a Postdoctoral Research Fellow with the Department of Electronics, Information and Bioengineering (DEIB), Politecnico di Milano. His research interests are in the field of optical networking, cloud computing, and optimization of communications networks.

FRANCESCO MUSUMECI (Member, IEEE) received the Ph.D. degree in information engineering from Politecnico di Milano, Italy, in 2013. He is currently an Assistant Professor with the Department of Electronics, Information and Bioengineering, Politecnico di Milano, since 2016. His current research interests include design, optimization and performance analysis of optical networks, applications of machine learning to networking, 5G, network function virtualization, and network disaster resilience. He is author of more than 80 papers in the area of communication networks, published in international journals and conference proceedings, and is co-winner of three best paper awards from IEEE sponsored conferences. He used to serve as a TPC member and/or reviewer for several IEEE/OSA conferences as well as IEEE/OSA and Elsevier journals since 2010.

MASSIMO TORNATORE (Senior Member, IEEE) is currently an Associate Professor with the Department of Electronics, Information, and Bioengineering, Politecnico di Milano. He also holds an appointment as an Adjunct Professor with the University of California, Davis, USA, and as a Visiting Professor with the University of Waterloo, Canada. His research interests include performance evaluation, optimization and design of communication networks (with an emphasis on the application of optical networking technologies), cloud computing, and machine learning application for network management. In these areas, he coauthored more than 350 peer-reviewed conference and journal papers (with 18 best paper awards), two books, and one patent. He is a member of the Editorial Board of the IEEE COMMUNICATION SURVEYS AND TUTORIALS, IEEE COMMUNICATION LETTERS, *Springer Photonic Network Communications, and Elsevier Optical Switching and Networking*. He is active member of the technical program committee of various networking conferences such as INFOCOM, OFC, ICC, and GLOBECOM. He acted as technical program chair of ONDM 2016 and DRCN 2017 and DRCN 2019 conferences. He has participated in several EU R&D projects (among others FP7 COMBO, H2020 MetroHaul, and Cost Action RECODIS) as well as in several projects in USA, Canada, and Italy.

